Quantum Chemical and Kinetic Study on Dioxin Formation from the 2,4,6-TCP and 2,4-DCP Precursors

QINGZHU ZHANG,* WANNI YU,
RUIXUE ZHANG, QIN ZHOU, RUI GAO,
AND WENXING WANG*

*Environment Research Institute, Shandong University,
Jinan 250100, P. R. China*

This study focuses on the homogeneous gas-phase formation of polychlorinated dibenzo-*p*-dioxins (PCDDs) and dibenzofurans (PCDFs) from the 2,4,6-trichlorophenol (2,4,6-TCP) and 2,4-dichlorophenol (2,4-DCP) precursors, which were found both in the gas phase and in the fly ash samples as the dominating chlorophenol congeners in municipal waste incinerators (MWIs). Molecular orbital theory calculations have been performed for the formation mechanism. The geometrical parameters and vibrational frequencies of all the stationary points were calculated at the MPWB1K level with the 6-31+G(d,p) basis set. Single-point energy calculations were carried out at the MPWB1K/6-311+G(3df,2p) level of theory. Canonical variational transition-state (CVT) theory with small curvature tunneling (SCT) contribution was used to predict the rate constants of crucial elementary steps over the temperature range of interest (600−1200 K). The rate-temperature formulas were fitted for the first time. The pre-exponential factor, the activation energy, and the rate constants are reported. This study shows that at least one chlorine substituent in the ortho position is needed for the formation of PCDDs from the condensation of chlorophenols. The results presented here should help to clarify and detail the formation mechanism of PCDD/PCDFs (PCDD/Fs for short) from chlorophenol precursors in real waste combustion.

1. Introduction

Polychlorinated dibenzo-*p*-dioxins (PCDDs) and dibenzofurans (PCDFs) are a constant concern from the environmental point of view due to their extreme toxicity, bioaccumulation and persistency in the environment (*1*). In particular, surprisingly high levels of PCDD/PCDFs (PCDD/Fs for short) were even observed in polar region (*2*). The origin and formation mechanism of PCDD/Fs continue to be heavily debated and researched. Combustion processes, especially those of municipal solid waste, are important sources of PCDD/Fs (*3*). Chlorophenols (CPs) are structurally similar to PCDD/Fs and among the most abundant aromatic compounds found in municipal waste incinerators (MWIs) flue gases (*4−6*). Chlorophenols have been demonstrated to be the predominant precursors of PCDD/Fs in MWIs (*7, 8*). The homogeneous gas-phase formation of PCDD/Fs from chlorophenol precursors was suggested to make a significant contribution to the observed PCDD/F yields in full-scale incinerators (*9−12*).

Chlorophenols are a broad range of contaminants released from direct application as biocides, leaching from wood products, synthesis during bleaching operations, and emissions from operating facilities (*13−15*). Due to the different chlorine substitution patterns, chlorophenols have 19 congeners. Thereinto, pentachlorophenol (PCP), 2,3,4,6-tetrachlorophenol (2,3,4,6-TeCP), 2,4,6-trichlorophenol (2,4,6-TCP), 2,4-dichlorophenol (2,4-DCP), and 2-chlorophenol (2-CP) are the most abundant congeners found in municipal waste incinerators (*16, 17*). In the respective homologue groups they contribute more than 90% to the total concentration (*18*). The PCDDs, which are formed by dimerization of the above five chlorophenols, represent more than 90% of the total PCDD concentration (*18*). An understanding of the elementary processes that govern the formation of PCDD/Fs is needed to elucidate and control their formation. In the recently published studies (*19, 20*), we investigated the formation of PCDD/Fs from the 2,4,5-TCP and 2-CP precursors (2,4,5-TCP has the minimum number of Cl atoms needed to form 2,3,7,8-TeCDD, which is the most toxic among all 210 PCDD/F congeners). In this article, we report the quantum chemical and kinetic studies on the formation of PCDD/Fs from the 2,4,6-TCP and 2,4-DCP precursors. A detailed reaction mechanism accounting for all reported products is proposed. More possible PCDD formation pathways were revealed in this work compared with those reported in the previous studies (*19, 20*).

The work was stimulated by several motivations. First, 2,4,6-TCP is widely used as an antiseptic, a pesticide for wood, leather, and glue preservation, and as an antimildew treatment. 2,4-DCP is used extensively in the manufacture of pesticides and herbicides. High concentrations were found in exhaust gases emitted from municipal waste incinerators (*18*). Second, 2,4,6-TCP and 2,4-DCP are the most reactive to form PCDDs (*21*). For example, 1,3,6,8-TeCDD and 1,3,7,9-TeCDD, the most abundant PCDD congeners found in municipal waste incinerator, are produced by dimerization of 2,4,6-TCP (*18, 21*). Third, the PCDD/F formation mechanism from the 2,4,6-TCP and 2,4-DCP precursors are not yet completely understood in spite of the fact that several laboratory studies have been conducted under various experimental conditions (*22, 23*). According to the mechanism proposed for 2,4,5-TCP and 2-CP (*19, 20*), only a single PCDD isomer, 1,3,6,8-TeCDD, can be produced from 2,4,6-TCP due to its symmetry. However, two isomers, 1,3,6,8-TeCDD and 1,3,7,9-TeCDD, in near-equal yield were experimentally observed (*22*). How can the formation of 1,3,7,9-TeCDD be explained? Fourthly, regulatory decisions and risk analyses often rely on the use of mathematical models to predict the potential outcomes of contaminant releases to the environment. In most of the kinetic models of the PCDD/F formation, 2,4,6-TCP was selected as a model precursor (*10, 22, 24, 25*). However, due to the absence of direct experimental and theoretical values, the rate constants of many elementary steps were assigned to be the values reported in the literature for analogous reactions (*10, 22, 24, 25*). For example, the rate constant for 2,4,6-TCP + OH → 2,4,6-TCPR + H₂O was assigned to be the values for $C_6H_5OH + OH \rightarrow C_6H_5O + H_2O$ (*10, 24*). The rate coefficient for the following elementary step was assigned by analogy with the reaction of $CH_3Cl + H \rightarrow CH_2Cl + H_2$ (*10, 24*). However, where there are uncertainties, the numerical values have been adjusted somewhat to bias the mechanism in favor of PCDD/Fs formation, i.e., worst case modeling (*10*).

* Corresponding author fax: 86-531-8836 1990; e-mail: zqz@sdu.edu.cn.
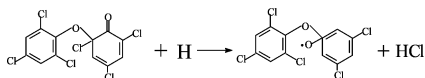
2. Computational Methods

All of the electronic structure calculations were carried out with the Gaussian 03 suite of programs (*26*) on an SGI 2000 supercomputer. As a reasonable compromise between accuracy and computational time, the geometries of the stationary points were fully optimized by employing the MPWB1K method (*27*) with a standard 6-31+G(d,p) basis set. Based on the modified Perdew and Wang exchange functional (MPW) and Becke's 1995 correlation functional (B95), MPWB1K is an excellent method for prediction of transition state geometries and thermochemical kinetics. The harmonic vibrational frequencies were calculated at the same level. Unscaled vibrational frequencies were employed for the calculation of zero-point energy (ZPE) corrections, the characterization of stationary points, and rate constant calculations. All the stationary points have been identified for local minima and transition state by vibrational analysis. The minimum energy path (MEP) was obtained by the intrinsic reaction coordinate (IRC) theory to confirm that the transition state really connects to minima along the reaction path. Also, first and second energy derivatives at geometries along the MEP were obtained to calculate the curvature of the reaction path and to calculate the generalized vibrational frequencies along the reaction path. To acquire more reliable kinetic information, a more flexible basis set, 6-311+G(3df,2p), was employed to determine the energies of the various species. The reliability of the MPWB1K/6-311+G(3df,2p) level for the potential barriers has been clarified in our recent study on the formation of PCDD/Fs from the 2-CP precursor (*20*). All the relative energies quoted and discussed in this paper include ZPE corrections with unscaled frequencies obtained at the MPWB1K/6-31+G(d,p) level.

Dynamic calculations were performed using the Polyrate 9.3 program (*28*). Canonical variational transition-state theory (*29−31*) with the small-curvature tunneling (SCT) (*32*) contribution was applied to evaluate the theoretical rate constants. The CVT rate constant for temperature T is given by

$$k^{CVT}(T) = \min_s k^{GT}(T, s) \qquad (1)$$

where

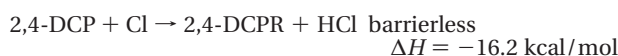$$k^{GT}(T, s) = \frac{\sigma k_B T}{h} \frac{Q^{GT}(T, s)}{\Phi^R(T)} e^{-V_{MEP}(s)/k_B T} \qquad (2)$$
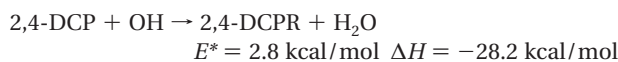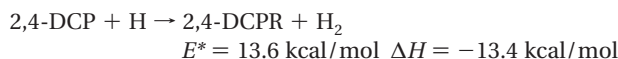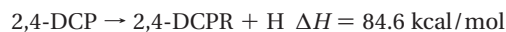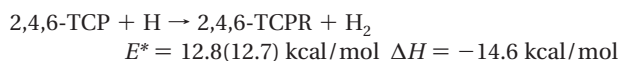
where $k^{GT}(T,s)$ is the generalized transition state theory rate constant at the dividing surface s, σ is the symmetry factor accounting for the possibility of more than one symmetry-related reaction path, k_B is Boltzmann's constant, h is Planck's constant, $\Phi^R(T)$ is the reactant partition function per unit volume, excluding symmetry numbers for rotation, and $Q^{GT}(T, s)$ is the partition function of a generalized transition state at s with a local zero of energy at $V_{MEP}(s)$ and with all rotational symmetry numbers set to unity. The rotational partition functions were calculated classically, and the vibrational modes were treated as quantum-mechanically separable harmonic oscillators.

3. Results and Discussion

3.1. Formation of 2,4,6-TCPRs and 2,4-DCPRs.
Previous works (*33, 34*) have shown that the dimerization of chlorophenoxy radicals (CPRs) is the dominant pathway in the gas-phase formation of PCDD/Fs from chlorophenol pre-cursors. The formation of chlorophenoxy radicals is the initial step in the formation of PCDD/Fs. In municipal waste incinerators, chlorophenoxy radicals can be produced through loss of the phenoxyl-hydrogen via unimolecular, bimolecular, or possibly other low-energy pathways (including heterogeneous reactions). The unimolecular reaction includes the decomposition of chlorophenols with the cleavage of the O−H bond. The bimolecular reactions include the phenolic-hydrogen abstraction from chlorophenols by the active radicals H, OH, O (^{3}P), and Cl, which are abundant in the combustion environment. At temperatures greater than 900 K, the former is dominant. Below 900 K, the latter becomes important. The sources and formation mechanism of H, OH, O (^{3}P), and Cl in the combustion environment were described in detail in the literature (*10, 35, 36*).

The potential barriers (E^*, include the ZPE correction) and the reaction heats (ΔH, include the ZPE correction) were calculated at the MPWB1K/6-311+G(3df,2p)//MPWB1K/6-31+G(d,p) level. In particular, the energies of the transition states without the ZPE correction are higher than the total energies of the separated reactants for the reactions of 2,4,6-TCP and 2,4-DCP with Cl, respectively. However, the energies of the transition states with the ZPE correction are lower than the total energies of the separated reactants. So, the two reactions should occur with no barrier. In order to justify the performance of the MPWB1K method for the potential barriers of phenolic-hydrogen abstraction reactions, we have also carried out additional potential barrier calculations employing the BB1K/6-311+G(3df,2p)//BB1K/6-31+G(d,p) method for the phenoxyl-hydrogen abstraction for 2,4,6-TCP. The two methods, MPWB1K/6-311+G(3df,2p)//MPWB1K/6-31+G(d,p) and BB1K/6-311+G(3df,2p)//BB1K/6-31+G(d,p), produce consistent potential barriers within 0.2 kcal/mol. The values in parentheses are the potential barriers calculated at the BB1K/6-311+G(3df,2p)//BB1K/6-31+G(d,p) level, and the values out of parentheses are the potential barriers obtained at the MPWB1K/6-311+G(3df,2p)//MPWB1K/6-31+G(d,p) level.

2,4,6-TCP → 2,4,6-TCPR + H ΔH = 83.3 kcal/mol

2,4,6-TCP + H → 2,4,6-TCPR + H$_2$
E^* = 12.8(12.7) kcal/mol ΔH = −14.6 kcal/mol

2,4,6-TCP + OH → 2,4,6-TCPR + H$_2$O
E^* = 2.7(2.9) kcal/mol ΔH = −29.5 kcal/mol

2,4,6-TCP + O(^{3}P) → 2,4,6-TCPR + OH
E^* = 6.9(7.0) kcal/mol ΔH = −14.0 kcal/mol

2,4,6-TCP + Cl → 2,4,6-TCPR + HCl
barrierless(barrierless) ΔH = −17.6 kcal/mol

2,4-DCP → 2,4-DCPR + H ΔH = 84.6 kcal/mol

2,4-DCP + H → 2,4-DCPR + H$_2$
E^* = 13.6 kcal/mol ΔH = −13.4 kcal/mol

2,4-DCP + OH → 2,4-DCPR + H$_2$O
E^* = 2.8 kcal/mol ΔH = −28.2 kcal/mol

2,4-DCP + O(^{3}P) → 2,4-DCPR + OH
E^* = 7.1 kcal/mol ΔH = −12.6 kcal/mol

2,4-DCP + Cl → 2,4-DCPR + HCl barrierless
ΔH = −16.2 kcal/mol

3.2. Formation of PCDD/Fs from 2,4,6-TCPRs and 2,4-DCPRs.
3.2.1. Formation of PCDDs from 2,4,6-TCPRs and 2,4-DCPRs. Two PCDD isomers, 1,3,6,8 and 1,3,7,9 tetrachlorodibenzo-*p*-dioxins (1,3,6,8-TeCDD and 1,3,7,9-TeCDD), were experimentally observed at temperatures
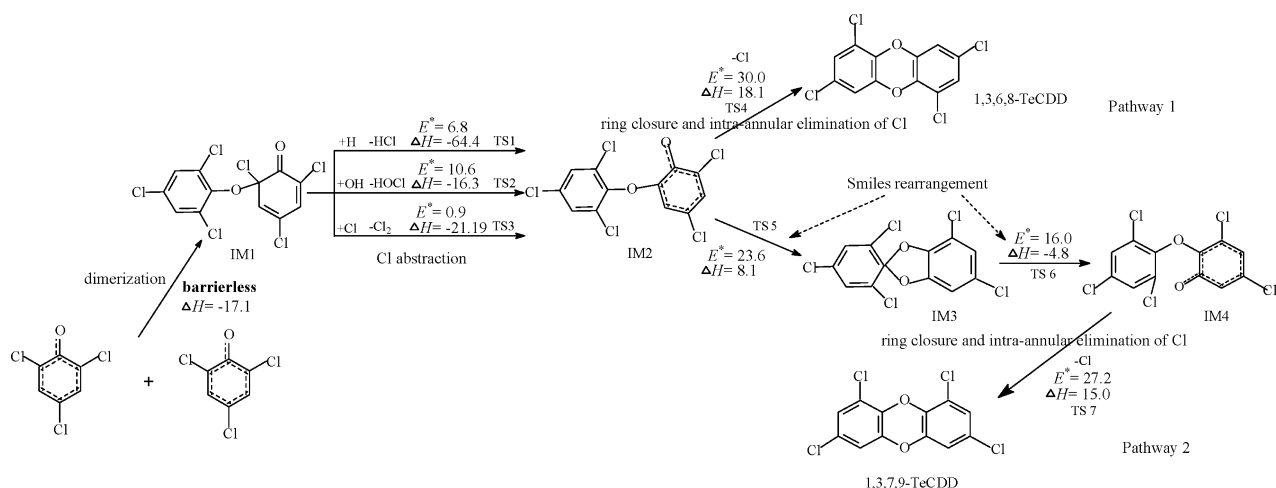
FIGURE 1. PCDD formation routes embedded with the potential barriers *E** (in kcal/mol) and reaction heats ΔH (in kcal/mol) from the 2,4,6-TCP precursor. ΔH is calculated at 0 K.
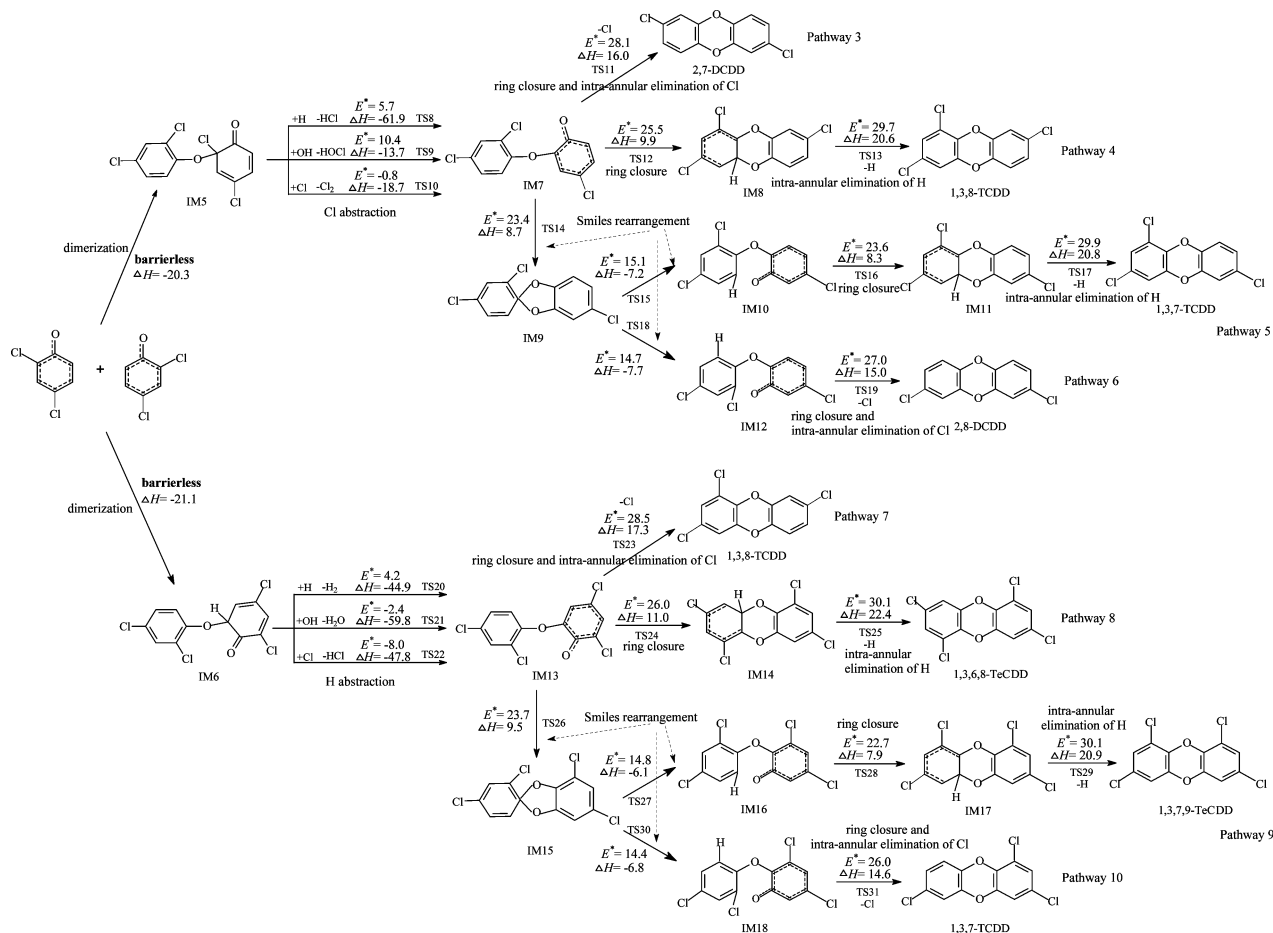

FIGURE 2. PCDD formation routes embedded with the potential barriers *E** (in kcal/mol) and reaction heats ΔH (in kcal/mol) from the 2,4-DCP precursor. ΔH is calculated at 0 K.

above approximately 500 °C in the pyrolysis of 2,4,6-TCP (22). The formation schemes embedded with the potential barriers and reaction heats are depicted in Figure 1. As introduced in our recent studies (19, 20), PCDDs are formed via the *o*-phenoxy-phenol (POP) intermediate. Due to the high symmetry of 2,4,6-TCPR, only one POP intermediate, denoted as IM1, is come into being from the dimerization of 2,4,6-TCPRs via oxygen—carbon coupling. The formation of 1,3,6,8-TeCDD involves the following elementary processes: dimerization (oxygen—carbon coupling) of 2,4,6-

TCPRs, Cl abstraction (The Cl atom in IM1 is abstracted by H, OH, or Cl.), ring closure, and intra-annular elimination of Cl. The dimerization of 2,4,6-TCPRs appears to be barrierless and strongly exothermic. The Cl abstraction step is highly exothermic with a trivial barrier. The ring closure and intra-annular elimination of Cl occur in a one-step reaction through the transition state TS4. This elementary process requires a high potential barrier of 30.0 kcal/mol and is strongly endoergic by 18.1 kcal/mol, and it is the rate determining step. The formation of 1,3,7,9-
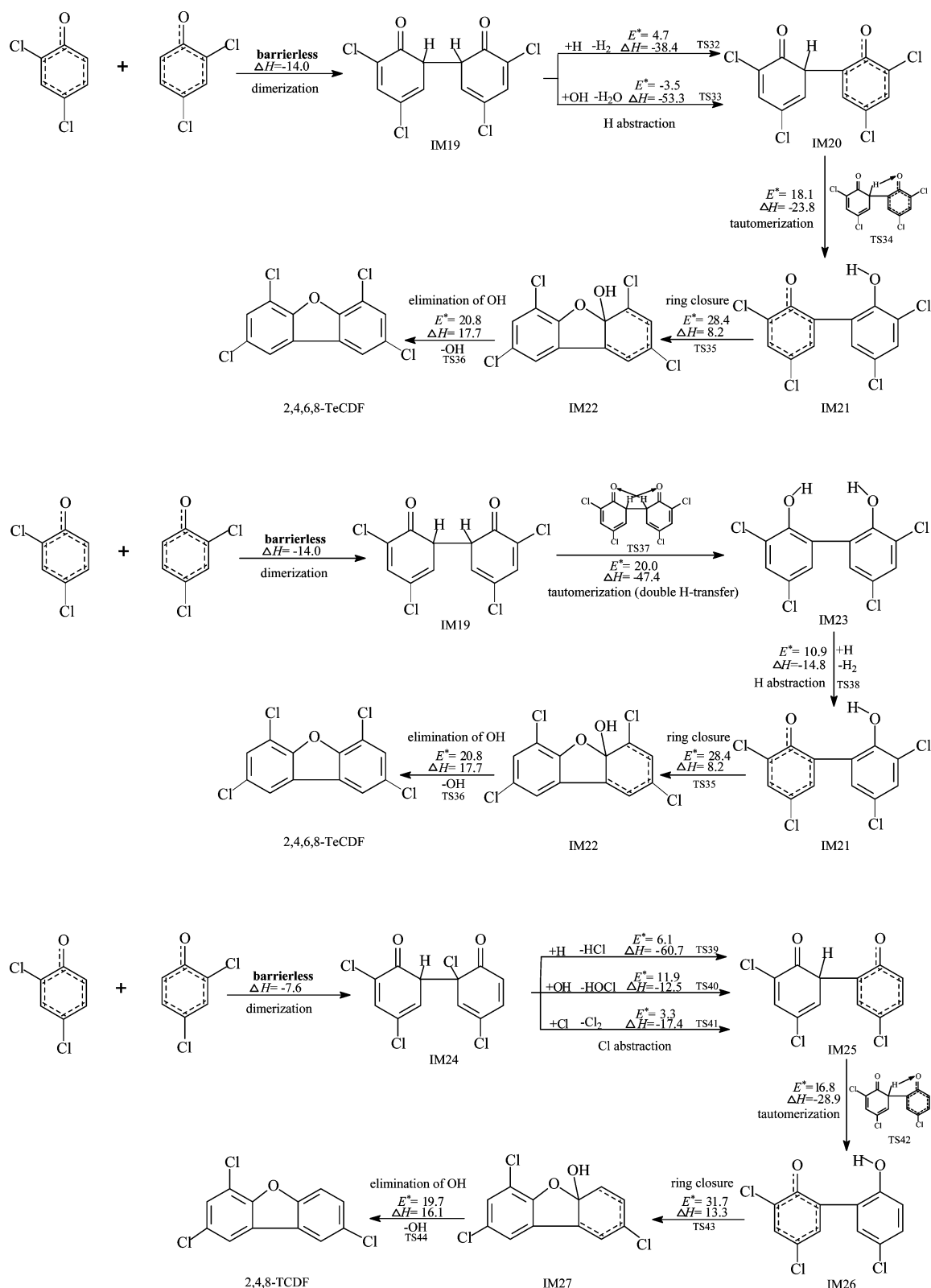
FIGURE 3. PCDF formation routes embedded with the potential barriers E^* (in kcal/mol) and reaction heats ΔH (in kcal/mol) from the 2,4-DCP precursor. ΔH is calculated at 0 K.

TeCDD includes five elementary processes: dimerization of 2,4,6-TCPRs, Cl abstraction, Smiles rearrangement (two elementary steps), ring closure, and intra-annular elimination of Cl (They occur in a one-step reaction and are the rate determining step.). The Smiles rearrangement (37) is an intramolecular nucleophilic aromatic substitution of the type:
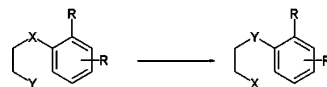
Clearly, the formation of 1,3,7,9-TeCDD involves two more elementary steps (Smiles rearrangement) compared with the formation of 1,3,6,8-TeCDD. It appears that the

TABLE 1. Arrhenius Formulas (Units Are s⁻¹ and cm³ molecule⁻¹ s⁻¹ for Unimolecular and Bimolecular Reactions, Respectively) for Elementary Reactions Involved in the Formation of PCDDs from the 2,4,6-TCP Precursor over the Temperature Range of 600−1200 K

reactions	Arrhenius formulas
2,4,6-TCP + H → 2,4,6-TCPR + H$_2$	$k(T) = (2.61 \times 10^{-12}) \exp(-6393.4/T)$
2,4,6-TCP + OH → 2,4,6-TCPR + H$_2$O	$k(T) = (9.58 \times 10^{-13}) \exp(-2752.8/T)$
2,4,6-TCP + O(^{3}P) → 2,4,6-TCPR + OH	$k(T) = (7.40 \times 10^{-11}) \exp(-4730.0/T)$
2,4,6-TCP + Cl → 2,4,6-TCPR + HCl	$k(T) = (2.23 \times 10^{-10}) \exp(-983.2/T)$
IM1 + H → IM2 + HCl	$k(T) = (3.01 \times 10^{-11}) \exp(-3981.2/T)$
IM1 + OH → IM2 + HOCl	$k(T) = (1.98 \times 10^{-11}) \exp(-10541.2/T)$
IM1 + Cl → IM2 + Cl$_2$	$k(T) = (7.09 \times 10^{-11}) \exp(-1905.7/T)$
IM2 → 1,3,6,8-TeCDD + Cl	$k(T) = (5.52 \times 10^{10}) \exp(-12386.7/T)$
IM2 → IM3	$k(T) = (3.07 \times 10^{12}) \exp(-9365.3/T)$
IM3 → IM4	$k(T) = (1.70 \times 10^{13}) \exp(-8569.5/T)$
IM4 → 1,3,7,9-TeCDD + Cl	$k(T) = (5.25 \times 10^{11}) \exp(-13581.6/T)$

formation of 1,3,6,8-TeCDD is preferred over the formation of 1,3,7,9-TeCDD. However, the rate determining step involved in the formation of 1,3,6,8-TeCDD requires crossing a higher barrier and is more endothermic than that involved in the formation of 1,3,7,9-TeCDD. This comparatively low barrier of the rate determining step is favored in the formation of 1,3,7,9-TeCDD. In addition, the two PCDD isomers are almost identical in energy. Taking one with another, the formations of 1,3,6,8-TeCDD and 1,3,7,9-TeCDD should be competitive. The calculated result is supported by the experimental observation that almost equal yields were measured for 1,3,6,8-TeCDD and 1,3,7,9-TeCDD in the pyrolysis of 2,4,6-TCP (22).

Due to the asymmetric chlorine substitution, relative more PCDD congeners can be produced from the 2,4-DCP precursor compared with those formed from the 2,4,6-TCP precursor. The formation mechanism is displayed in Figure 2. It is clear from Figure 2 that pathway 3 is similar to pathway 7, which involves three elementary processes: dimerization of 2,4-DCPRs, Cl or H abstraction (The Cl atom in IM5 or the H atom in IM6 is abstracted by H, OH, or Cl.), ring closure, and intra-annular elimination of Cl. The ring closure and intra-annular elimination of Cl are found to occur in one step and are the rate determining step. Pathway 4 and pathway 8 are homologous, and they include four elementary steps: dimerization of 2,4-DCPRs, Cl or H abstraction, ring closure, and intra-annular elimination of H. The intra-annular elimination of H is the rate determining step. Pathway 5 is

analogous to pathway 9, which covers six elementary processes: dimerization of 2,4-DCPRs, Cl or H abstraction, Smiles rearrangement (two elementary steps), ring closure, and intra-annular elimination of H (the rate determining step). Pathway 6 and pathway 10 are similar, and they contain five elementary processes: dimerization of 2,4-DCPRs, Cl or H abstraction, Smiles rearrangement (two elementary steps), ring closure, and intra-annular elimination of Cl (The ring closure and intra-annular elimination of Cl occur in a one-step reaction and are the rate determining step.). Obviously, pathway 3 involves relative less elementary steps compared with pathway 4 and pathway 5, respectively. Furthermore, the rate determining step involved in pathway 3 has a lower potential barrier and is less endoergic than that involved in pathway 4 and pathway 5, respectively. So, pathway 3 is preferred over pathway 4 and pathway 5, respectively. For the same reason, pathway 7 is preferred over pathway 8 and pathway 9, respectively. Pathway 6 includes two more elementary steps than pathway 3. However, the rate determining step involved in pathway 3 requires a higher barrier and is more endothermic than that involved in pathway 6. So, pathway 3 and pathway 6 should be competitive. Similarly, pathway 7 and pathway 10 are competitive. Thus, the thermodynamically favored routes to the PCDD formations from the 2,4-DCP precursor are pathway 3, pathway 6, pathway 7, and pathway 10. The resulting 2,7-DCDD, 2,8-DCDD, 1,3,8-TCDD, and 1,3,7-TCDD are the main PCDD products. This is consistent with the experimental observation: large amounts

TABLE 2. Arrhenius Formulas (Units Are s^{-1} and cm^3 molecule^{-1} s^{-1} for Unimolecular and Bimolecular Reactions, Respectively) for Elementary Reactions Involved in the Formation of PCDDs from the 2,4-DCP Precursor over the Temperature Range of 600−1200 K

reactions	Arrhenius formulas
2,4-DCP + H → 2,4-DCPR + H$_2$	$k(T) = (5.01 \times 10^{-11}) \exp(-7238.7/T)$
2,4-DCP + OH → 2,4-DCPR + H$_2$O	$k(T) = (3.43 \times 10^{-12}) \exp(-2948.9/T)$
2,4-DCP + O(^{3}P) → 2,4-DCPR + OH	$k(T) = (6.51 \times 10^{-11}) \exp(-4988.4/T)$
2,4-DCP + Cl → 2,4-DCPR + HCl	$k(T) = (7.75 \times 10^{-11}) \exp(-1573.0/T)$
IM5 + OH → IM7 + HOCl	$k(T) = (2.91 \times 10^{-11}) \exp(-6617.0/T)$
IM5 + Cl → IM7 + Cl$_2$	$k(T) = (8.94 \times 10^{-11}) \exp(-1293.2/T)$
IM7 → 2,7-DCDD	$k(T) = (2.44 \times 10^{9}) \exp(-12940.3/T)$
IM7 → IM8	$k(T) = (5.66 \times 10^{10}) \exp(-12555.1/T)$
IM8 → 1,3,8-TCDD	$k(T) = (8.94 \times 10^{12}) \exp(-14388.0/T)$
IM7 → IM9	$k(T) = (1.41 \times 10^{12}) \exp(-11703.5/T)$
IM9 → IM10	$k(T) = (2.79 \times 10^{12}) \exp(-6450.5/T)$
IM10 → IM11	$k(T) = (3.59 \times 10^{11}) \exp(-11649.4/T)$
IM11 → 1,3,7-TCDD + H	$k(T) = (3.86 \times 10^{13}) \exp(-15813.7/T)$
IM9 → IM12	$k(T) = (4.60 \times 10^{12}) \exp(-7401.2/T)$
IM12 → 2,8-DCDD + Cl	$k(T) = (6.48 \times 10^{10}) \exp(-13762.9/T)$
IM6 + H → IM13 + H$_2$	$k(T) = (1.65 \times 10^{-11}) \exp(-2323.8/T)$
IM13 → 1,3,8-TCDD + Cl	$k(T) = (5.28 \times 10^{11}) \exp(-14332.4/T)$
IM13 → IM14	$k(T) = (5.60 \times 10^{11}) \exp(-12945.6/T)$
IM14 → 1,3,6,8-TeCDD + H	$k(T) = (3.17 \times 10^{13}) \exp(-15877.4/T)$
IM13 → IM15	$k(T) = (1.26 \times 10^{12}) \exp(-11828.3/T)$
IM15 → IM16	$k(T) = (2.91 \times 10^{-11}) \exp(-6617.0/T)$

TABLE 2. Continued

reactions	Arrhenius formulas
IM16 → IM17	$k(T) = (1.85 \times 10^{11}) \exp(-11222.1/T)$
IM17 → 1,3,7,9-TeCDD + H	$k(T) = (2.96 \times 10^{13}) \exp(-15809.2/T)$
IM15 → IM18	$k(T) = (3.25 \times 10^{11}) \exp(-4806.5/T)$
IM18 → 1,3,7-TCDD + Cl	$k(T) = (5.02 \times 10^{11}) \exp(-13802.3/T)$

TABLE 3. Arrhenius Formulas (Units Are s^{-1} and cm^3 molecule^{-1} s^{-1} for Unimolecular and Bimolecular Reactions, Respectively) for Elementary Reactions Involved in the Formation of PCDFs from the 2,4-DCP Precursor over the Temperature Range of 600−1200 K

reactions	Arrhenius formulas
IM19 + H → IM20 + H$_2$	$k(T) = (5.34 \times 10^{-13}) \exp(-2544.1/T)$
IM19 + OH → IM20 + H$_2$O	$k(T) = (1.68 \times 10^{-12}) \exp(288.3/T)$
IM20 → IM21	$k(T) = (8.04 \times 10^{9}) \exp(-2160.3/T)$
IM21 → IM22	$k(T) = (1.91 \times 10^{9}) \exp(-5455.0/T)$
IM22 → 2,4,6,8-TeCDF + OH	$k(T) = (3.17 \times 10^{13}) \exp(-10982.1/T)$
IM19 → IM23	$k(T) = (2.62 \times 10^{9}) \exp(-3951.5/T)$
IM23 + H → IM21 + H$_2$	$k(T) = (2.79 \times 10^{-12}) \exp(-6004.5/T)$
IM24 + H → IM25 + HCl	$k(T) = (8.49 \times 10^{-13}) \exp(-1841.5/T)$
IM24 + OH → IM25 + HOCl	$k(T) = (1.16 \times 10^{-12}) \exp(-7167.2/T)$
IM24 + Cl → IM25 + Cl$_2$	$k(T) = (2.53 \times 10^{-12}) \exp(-3353.4/T)$
IM25 → IM26	$k(T) = (3.94 \times 10^{9}) \exp(-2444.0/T)$
IM26 → IM27	$k(T) = (5.79 \times 10^{12}) \exp(-16176.4/T)$
IM27 → 2,4,8-TCDF + OH	$k(T) = (2.83 \times 10^{13}) \exp(-10336.5/T)$

of 2,7-DCDD, 2,8-DCDD, 1,3,8-TCDD, and 1,3,7-TCDD were observed, but 1,3,6,8-TeCDD and 1,3,7,9-TeCDD were not detected in the pyrolysis of 2,4-DCP (23).

Comparison of the formation mechanism of PCDDs from the 2,4,6-TCP, 2,4,5-TCP, 2,4-DCP, and 2-CP precursors (19, 20) shows that the rate determining step is intra-annular

elimination of Cl or H. The intra-annular elimination of H requires crossing a higher barrier and is more endothermic compared with the intra-annular elimination of Cl. The thermodynamically preferred routes to the PCDD formations proceed through intra-annular elimination of Cl. The Cl atom, which is eliminated, is the substituent at the ortho position in chlorophenol. This can explain the experimental observation that only chlorophenols with chlorine at the ortho position are capable of forming PCDDs (23). This can also explain the experimental phenomena that for a given chlorophenol precursor with n chlorine atoms (at least one Cl substituent at the ortho position), only $P_{2n-1}CDD$ and/or $P_{2n-2}CDD$ can be produced, but no formation of $P_{2n}CDD$ is observed (23). The substitution pattern of chlorophenols not only determines the substitution pattern of the resulting PCDDs but also has a significant influence on the formation mechanism. For example, the oxygen−carbon coupling of 2,4,6-TCPR is less exothermic compared with the oxygen−carbon couplings of 2,4,5-TCPR and 2,4-DCPR, respectively. This is probably due to the steric hindrance during the formation of the POP if both ortho-positions of phenol are substituted with chlorine atoms.

3.2.2. Formation of PCDFs from 2,4-DCPRs. Previous research has shown that the formation of PCDFs were based primarily on ortho−ortho coupling of chlorophenoxy radicals to form an intermediate of *o,o′*-dihydroxybiphenyl (DOHB) (23). The sterically demanding formation of DOHB is inhibited by the voluminous chlorine atoms. If both ortho-positions of phenol are substituted with chlorine, the formation of PCDFs is completely inhibited (23). So, no PCDFs can be produced from the dimerization of 2,4,6-TCP (22, 23). Two DOHB intermediates, denoted as IM19 and IM24, are formed from the ortho−ortho coupling of 2,4-DCPRs. Thus, two PCDF congeners, 2,4,6,8-tetrachlorinated dibenzofuran (2,4,6,8-TeCDF) and 2,4,8-trichlorinated dibenzofuran (2,4,8-TCDF), can be produced from the 2,4-DCP precursor. The formation pathways are presented in Figure 3.

Two formation routes are proposed for 2,4,6,8-TeCDF. The first one involves five elementary steps: dimerization of 2,4-DCPRs (carbon−carbon coupling), H abstraction, tautomerization (H-shift), ring closure, and elimination of OH. The ring closure process has a large barrier, is strongly endoergic, and is the rate determining step. The second formation pathway of 2,4,6,8-TeCDF also includes five elementary processes: dimerization of 2,4-DCPRs, tautomerization (double H-transfer), H abstraction, ring closure (the rate determining step), and OH desorption. IM24 cannot isomerize via double H-transfer. So, only one possible formation pathway, depicted in Figure 3, is proposed for 2,4,8-TCDF.

3.3. Rate Constant Calculations. The rate constants of the elementary reactions involved in the formation of PCDD/Fs from the 2,4,6-TCP and 2,4-DCP precursors were evaluated by canonical variation transition-state (CVT) theory over a wide temperature region from 600 to 1200 K. Quantum tunneling effect is calculated by means of the small curvature tunneling (SCT) method, based on the centrifugal-dominant small-curvature semiclassical adiabatic ground-state approximation. The CVT/SCT method has been successfully performed for the elementary reactions involved in the formation of PCDD/Fs from the 2,4,5-TCP and 2-CP precursors (19, 20).

The reliability of the CVT/SCT method was clarified in our recent studies (19, 20, 38). The CVT/SCT rate constants of $C_6H_5OH + H \rightarrow C_6H_5O + H_2$ are in good agreement with the corresponding experimental values (38), respectively. The CVT/SCT rate constants for 2,4,6-TCP + H → 2,4,6-TCPR + H_2 and 2,4-DCP + H → 2,4-DCPR + H_2 are over 1 order of magnitude smaller than the value of $C_6H_5OH + H \rightarrow C_6H_5O + H_2$ (38), respectively. At the MPWB1K/6-311 + G(3df,2p)

level, the potential barriers of 2,4,6-TCP + H → 2,4,6-TCPR + H_2 and 2,4-DCP + H → 2,4-DCPR + H_2 are 12.8 and 14.0 kcal/mol, respectively, whereas the value for $C_6H_5OH + H \rightarrow C_6H_5O + H_2$ is 11.73 kcal/mol (38). The chlorine substitution at the ortho position in chlorophenols decreases the reactivity of the O−H bond (38). Thus, our CVT/SCT rate constants for 2,4,6-TCP + H → 2,4,6-TCPR + H_2, 2,4-DCP + H → 2,4-DCPR + H_2 are reasonable. Due to the absence of the available experimental values, it is difficult to make a direct comparison of the calculated CVT/SCT rate constants with the experimental values for the other elementary reactions. We hope that our CVT/SCT calculations may provide a good estimate for the elementary reactions involved in the formation of PCDD/Fs from the 2,4,6-TCP and 2,4-DCP precursors.

The DOHB intermediate IM19 can be regarded as a prestructure for 2,4,6,8-TeCDF, and IM24 is a prestructure of 2,4,8-TCDF. It is clear from Figure 3 that the formation of IM19 is more exothermic compared with the formation of IM24. Furthermore, the rate constants of the rate determining step involved in the formation of 2,4,6,8-TeCDF are larger than those of the rate determining step involved in the formation of 2,4,8-TCDF. Thus, the formation of 2,4,6,8-TeCDF is preferred over the formation of 2,4,8-TCDF. This is supported by the experimental observation that the yield of 2,4,6,8-TeCDF is larger than that of 2,4,8-TCDF (23). Comparison of the formation of PCDFs from the 2,4,5-TCP, 2,4-DCP, and 2-CP precursors shows that the substitution pattern of chlorophenols has an effect on the formation mechanism of PCDFs, especially on the ortho−ortho coupling of CPRs.

The calculated CVT/SCT rate constants are fitted, and Arrhenius formulas are given in Table 1 for 2,4,6-TCP and in Tables 2 and 3 for 2,4-DCP. The pre-exponential factor, the activation energy, and the rate constants can be obtained from these Arrhenius formulas. The results will assist in the construction of detailed kinetic models describing the formation of PCDD/Fs in combustion processes.

Supporting Information Available

All of the optimized geometries in terms of Cartesian coordinate for reactants, products, and transition states and the total energies (in a.u.), the zero point energies (ZPE, in a.u.), and the imaginary frequencies (in cm^{-1}) for the transition states. This material is available free of charge via the Internet at http://pubs.acs.org.

Literature Cited

(1) Schecter, A. *Dioxin and Health*; Plenum Press: New York, 1994.

(2) Hung, H.; Blanchard, P.; Poole, G.; Thibert, B.; Chiu, C. H. Measurement of particle-bound polychlorinated dibenzo-*p*-dioxins and dibenzofurans (PCDD/Fs) in Arctic air at Alert, Nunavat, Canada. *Atmos. Environ.* **2002**, *36* (6), 1041–1050.

(3) *Chlorinated dioxins and related compounds*; Hutzinger, O., Frei, R. W., Merian, E., Pocchiari, F., Eds.; Pergamon Press: New York, 1982.

(4) Ryu, J.; Mulholland, J. A.; Kim, D. H.; Takeuchi, M. Homologue and isomer patterns of polychlorinated dibenzo-*p*-dioxins and dibenzofurans from phenol precursors: comparison with municipal waste incinerator data. *Environ. Sci. Technol.* **2005**, *39* (12), 4398–4406.

(5) Shaub, W. M.; Tsang, W. Dioxin formation in incinerators. *Environ. Sci. Technol.* **1983**, *17* (12), 721–730.

(6) Altwicker, E. R. Relative rates of formation of polychlorinated dioxins and furans from precursor and de novo reactions. *Chemosphere* **1996**, *33* (10), 1897–1904.

(7) Karasek, F. W.; Dickson, L. C. Model studies of polychlorinated dibenzo-*p*-dioxin formation during municipal refuse incineration. *Science* **1987**, *237* (4816), 754–756.

(8) Milligan, M. S.; Altwicker, E. R. Chlorophenol reactions on fly ash. 1. Adsorption/desorption equilibria and conversion to polychlorinated dibenzo-*p*-dioxins. *Environ. Sci. Technol.* **1995**, *30* (1), 225–229.

(9) Babushok, V. I.; Tsang, W. Gas-phase mechanism for dioxin formation. *Chemosphere* **2003**, *51* (10), 1023–1029.

(10) Khachatryan, L.; Burcat, A.; Dellinger, B. An elementary reaction-kinetic model for the gas-phase formation of 1,3,6,8- and 1,3,7,9-tetrachlorinated dibenzo-*p*-dioxins from 2, 4,6-trichlorophenol. *Combust. Flame* **2003**, *132* (3), 406–421.

(11) Hung, H.; Buekens, A. Comparison of dioxin formation levels in laboratory gas-phase flow reactors with those calculated using the Shaub-Tsang mechanism. *Chemosphere* **1999**, *38* (7), 1595–1602.

(12) Babushok, V.; Tsang, W. *7th International Congress on Combustion By-Products: Origins, Fate, and Health Effects*; Research Triangle Park, NC, 2001; p 36.

(13) Wegman, R. C. C.; van der Broek, H. H. Chlorophenols in river sediment in the Netherlands. *Water Res.* **1983**, *17* (2), 227–230.

(14) Buisson, R. S. K.; Kirk, P. W. W.; Lester, J. N. Determination of chlorinated phenols in water, wastewater and wastewater sludge by capillary GC-ECD. *J. Chromatogr. Sci.* **1984**, *22* (8), 339–342.

(15) Galceran, M. T.; Jauregui, O. Determination of phenols in sea water by liquid chromatography with electrochemical detection after enrichment by using solid-phase extraction cartridges and disks. *Anal. Chim. Acta* **1995**, *304* (1), 75–84.

(16) Addink, R.; Cnubben, P. A. J. P.; Olie, K. Formation of polychlorinated dibenzo-*p*-dioxins/dibenzofurnans on fly ash from precursors and carbon model compounds. *Carbon* **1995**, *33* (10), 1463–1471.

(17) Cains, P. W.; Mccausland, L.; Fernandes, A. R.; Dyke, P. Polychlorinated dibenzo-*p*-dioxins and dibenzofurans formation in incineration: Effects of fly ash and carbon source. *Environ. Sci. Technol.* **1997**, *31* (3), 776–785.

(18) Weber, R.; Hagenmaier, H. PCDD/PCDF formation in fluidized bed incineration. *Chemosphere* **1999**, *38* (11), 2643–2654.

(19) Qu, X. H.; Wang, H.; Zhang, Q. Z.; Shi, X. Y.; Xu, F.; Wang, W. X. Mechanistic and kinetic studies on the homogeneous gas-phase formation of PCDD/Fs from 2,4,5-trichlorophenol. *Environ. Sci. Technol.* **2009**, *43* (11), 4068–4075.

(20) Zhang, Q. Z.; Li, S. Q.; Qu, X. H.; Wang, W. X. A quantum mechanical study on the formation of PCDD/Fs from 2-chlorophenol as precursor. *Environ. Sci. Technol.* **2008**, *42* (19), 7301–7308.

(21) Briois, C.; Ryan, S.; Tabor, D.; Touati, A.; Gullett, B. Formation of polychlorinated dibenzo-*p*-dioxins and dibenzofurans from a mixture of chlorophenols over fly ash: Influence of water vapor. *Environ. Sci. Technol.* **2007**, *41* (3), 850–856.

(22) Sidhu, S. S.; Maqsud, L.; Dellinger, B.; Mascolo, G. The homogeneous, gas-phase formation of chlorinated and brominated dibenzo-*p*-dioxin from 2,4,6-trichloro- and 2,4,6-tribromophenols. *Combust. Flame* **1995**, *100* (1−2), 11–20.

(23) Weber, R.; Hagenmaier, H. Mechanism of the formation of polychlorinated dibenzo-*p*-dioxins and dibenzofurans from chlorophenols in gas phase reactions. *Chemosphere* **1999**, *38* (3), 529–549.

(24) Khachatryan, L.; Asatryan, R.; Dellinger, B. Development of expanded and core kinetic models for the gas phase formation of dioxins from chlorinated phenols. *Chemosphere* **2003**, *52* (4), 695–708.

(25) Khachatryan, L.; Asatryan, R.; Dellinger, B. An elementary reaction kinetic model of the gas-phase formation of polychlorinated dibenzofurans from chlorinated phenols. *J. Phys. Chem. A* **2004**, *108* (44), 9567–9572.

(26) Frisch, M. J.; Trucks, G. W.; Schlegel, H. B.; Gill, P. W. M.; Johnson, B. G.; Robb, M. A.; Cheeseman, J. R.; Keith, T. A.; Petersson, G. A.; Montgomery, J. A.; Raghavachari, K.; Allaham, M. A.; Zakrzewski, V. G.; Ortiz, J. V.; Foresman, J. B.; Cioslowski, J.; Stefanov, B. B.; Nanayakkara, A.; Challacombe, M.; Peng, C. Y.; Ayala, P. Y.; Chen, W.; Wong, M. W.; Andres, J. L.; Replogle, E. S.; Gomperts, R.; Martin, R. L.; Fox, D. J.; Binkley, J. S.; Defrees, D. J.; Baker, J.; Stewart, J. P.; Head-Gordon, M.; Gonzales, C.; Pople, J. A. *GAUSSIAN 03*; Pittsburgh, PA, 2003.

(27) Zhao, Y.; Truhlar, D. G. Hybrid meta density functional theory methods for therochemistry, thermochemical kinetics, and noncovalent interactions: The MPW1B95 and MPWB1K models and comparative assessments for hydrogen bonding and van der waals interactions. *J. Phys. Chem. A* **2004**, *108* (33), 6908–6918.

(28) Steckler, R.; Chuang, Y. Y.; Fast, P. L.; Corchade, J. C.; Coitino, E. L.; Hu, W. P.; Lynch, G. C.; Nguyen, K.; Jackells, C. F.; Gu, M. Z.; Rossi, I.; Clayton, S.; Melissas, V.; Garrett, B. C.; Isaacson, A. D.; Truhlar, D. G. *POLYRATE Version 9.3*; University of Minnesota: Minneapolis, 2002.

(29) Baldridge, M. S.; Gordor, R.; Steckler, R.; Truhlar, D. G. Ab initio reaction paths and direct dynamics calculations. *J. Phys. Chem.* **1989**, *93* (13), 5107–5119.

(30) Gonzalez-Lafont, A.; Truong, T. N.; Truhlar, D. G. Interpolated variational transition-state theory: Practical methods for estimating variational transition-state properties and tunneling contributions to chemical reaction rates from electronic structure calculations. *J. Chem. Phys.* **1991**, *95* (12), 8875–8894.

(31) Garrett, B. C.; Truhlar, D. G. Generalized transition state theory. Classical mechanical theory and applications to collinear reactions of hydrogen molecules. *J. Phys. Chem.* **1979**, *83* (8), 1052–1079.

(32) Fernandez-Ramos, A.; Ellingson, B. A.; Garret, B. C.; Truhlar, D. G. Variational Transition State Theory with Multidimensional Tunneling. In *Reviews in Computational Chemistry*; Lipkowitz, K. B., Cundari, T. R., Eds.; Wiley-VCH: Hoboken, NJ, 2007.

(33) Evans, C. S.; Dellinger, B. Mechanisms of dioxin formation from the high-temperature oxidation of 2-chlorophenol. *Environ. Sci. Technol.* **2005**, *39* (1), 122–127.

(34) Altarawneh, M.; Dlugogorski, B. Z.; Kennedy, E. M.; Mackie, J. C. Quantum chemical investigation of formation of polychlorodibenzo-*p*-dioxins and dibenzofurans from oxidation and pyrolysis of 2-chlorophenol. *J. Phys. Chem. A* **2007**, *111* (13), 2563–2573.

(35) Procaccini, C.; Bozzelly, J. W.; Longwell, J. P.; Smith, K. A.; Sarofim, A. F. Presence of chlorine radicals and formation of molecular chlorine in the post-flame region of chlorocarbon combustion. *Environ. Sci. Technol.* **2000**, *34* (21), 4565–4570.

(36) Ritter, E. R.; Bozzelli, J. W. Kinetic study on thermal decomposition of chlorobenzene diluted in hydrogen. *J. Phys. Chem.* **1990**, *94* (6), 2493.

(37) Levy, A. A.; Rains, H. C.; Smiles, S. CCCCLII.—The rearrangement of hydroxy-sulphones. Part I. *J. Chem. Soc.* **1931**, 3264–3269.

(38) Zhang, Q. Z.; Qu, X. H.; Xu, F.; Shi, X. Y.; Wang, W. X. Mechanism and thermal rate constants for the complete series reactions of chlorophenols with H. *Environ. Sci. Technol.* **2009**, *43* (11), 4105–4112.